

Abundance analysis of s-process enhanced barium stars

Upakul Mahanta^{1,2}, Drisya Karinkuzhi³, Aruna Goswami³, Kalpana Duorah²

¹ Department of Physics, Bajali College, Pathsala, Assam, 781325, India; upakulmahanta@gmail.com

² Department of Physics, Gauhati University, Guwahati 781014, Assam, India; khowang56@yahoo.co.in

³ Indian Institute of Astrophysics, Koramangala, Bangalore 560034, India;

drisya@iiap.res.in, aruna@iiap.res.in

Accepted —; Received —; in original form :

ABSTRACT

Detailed chemical composition studies of stars with enhanced abundances of neutron-capture elements can provide observational constraints for neutron-capture nucleosynthesis studies and clues for understanding their contribution to the Galactic chemical enrichment. We present abundance results from high-resolution spectral analyses of a sample of four chemically peculiar stars characterized by s-process enhancement. High-Resolution spectra ($R \sim 42000$) of these objects spanning a wavelength range from 4000 to 6800 Å, are taken from the ELODIE archive. We have estimated the stellar atmospheric parameters, the effective temperature T_{eff} , the surface gravity $\log g$, and metallicity $[Fe/H]$ from local thermodynamic equilibrium analysis using model atmospheres. We report estimates of elemental abundances for several neutron-capture elements, Sr, Y, Zr, Ba, La, Ce, Pr, Nd, Sm, Eu and Dy. While HD 49641 and HD 58368 show $[Ba/Fe] \geq 1.16$ the other two objects HD 119650 and HD 191010 are found to be mild barium stars with $[Ba/Fe] \sim 0.4$. The derived abundances of the elements are interpreted on the basis of existing theories for understanding their origin and evolution.

Key words: stars: individual (HD 49641, HD 58368, HD 119650, HD 191010) - stars: Abundances - stars: chemically peculiar - stars: nucleosynthesis

1 INTRODUCTION

The origin and evolution of neutron-capture elements in our Galaxy still remain poorly understood. Detailed chemical composition of stars with atmospheres enriched with heavy elements can provide clues for better understanding. Barium stars along with CH stars and the more metal-poor analogs of CH stars, the Carbon-Enhanced Metal-Poor (CEMP)-s stars provide important targets. Barium stars, first identified as a distinct group of peculiar objects by Bidelman & Keenan (1951) are Pop I red giants with spectral class G to K. Their spectra show strong presence of singly ionized Ba II lines, indicating an overabundance of s-process elements. Variations in radial-velocity in barium stars was revealed by McClure et al. (1980) and further confirmed by McClure (1983, 1984) and Udry et al. (1998a,b). The binary nature of barium stars was established from the observed radial velocity variations that suggested presence of companions. The most accepted interpretation for the observed abundance patterns in barium stars is that, they acquired the enrichment of s-process nucleosynthesis from an AGB companion that later evolved to a white dwarf. Detailed abundance studies of barium stars are thus important for a better

understanding of the s-process mechanisms in AGB stars, as well as the mass transfer mechanisms in binary systems.

Present theories include two main types of mass transfer mechanisms for barium stars in binary systems, the Roche-lobe overflow (RLOF) and wind-accretion scenarios. In the RLOF scenario, for sufficiently close binaries containing a thermally pulsing AGB (TP-AGB) star, as the star expands past the Roche lobe the material which lies outside the lobe can fall off into the secondary object. In the wind accretion model of Boffin & Jorissen (1988), the authors have shown that for large orbital separation the contamination of Ba stars depends only upon the present value of orbital separation and mass of the white dwarf companion. Here part of matter are ejected through a wind by an AGB star and the system remain always detached. This is the more favoured channel for barium star formation. An intermediate regime in which some wind mass-transfer occurs before RLOF begins has also been suggested (Han et al. 1995). However, none of these models can explain all the physical and orbital properties of Ba stars. While RLOF scenario is not favourable as this terminates the TP-AGB and lessens the production of barium, preventing barium-star formation, the wind-accretion scenario does not explain the distribution

of eccentricities and periods of barium stars (Izzard et al. 2010). Further studies are necessary to have clearer pictures on these issues. As much insight about the origin and evolution of heavy elements and the evolved AGB companion can be obtained from the chemical composition studies of these objects, and, given the current number of abundance analyses available, (although gradually increasing but for limited number of heavy elements), detailed abundance studies of even one or two more objects represent a significant contribution.

In the present work we have undertaken to conduct a detailed chemical composition study for four peculiar stars listed in the barium stars catalogue of Lü (1991), based on high resolution spectra ($R \sim 42000$) and high S/N with > 100 at about 5500 \AA . Among these four stars two objects HD 49641 and HD 58368 are included in the list of ‘Certain Ba II stars’ and one object HD 119650 is included in the list of ‘Marginal Ba II stars’ of MacConnell et al. (1972). No detailed studies were available in literature for these objects until recently when these two objects, HD 49641 and HD 58368 are found to be included in the chemical composition studies of barium stars by Yang et al. (2016) and de Castro et al. (2016). As far as the heavy element abundances are concerned, Yang et al. (2016) have reported abundances for five heavy elements (Y, Zr, Ba, La and Eu); likewise de Castro et al. (2016) have also reported on abundances of five heavy elements (Y, Zr, La, Ce, Nd). We have presented abundances for eleven neutron-capture elements and compared and contrast our results for these two objects with the results of the above two studies whenever possible. The other two objects, hitherto not studied, are found to be mild barium stars with $[\text{Ba}/\text{Fe}] \sim 0.4$.

In section 2 we have presented a brief summary on the chemical composition studies on HD 49641 and HD 58368 by Yang et al. (2016) and de Castro et al. (2016). In section 3 we have presented the details of the high resolution spectra used in this study. Photometric temperatures of the stars and the radial velocity estimates are also presented in this section. Section 4 describes briefly the methodology used for deriving the stellar atmospheric parameters. Error analysis is presented in section 5. Estimation of chemical abundances and the analysis of the abundance results are discussed in Section 6. Conclusions are presented in Section 7.

2 PREVIOUS STUDIES ON HD 49641 AND HD 58368: A SUMMARY

Some aspects of these two objects were addressed by Yang et al. (2016) and de Castro et al. (2016); here we summarize their main results.

Yang et al. (2016): These two objects were included in their chemical abundance studies of 19 barium stars. They have determined the stellar atmospheric parameters using red spectra in the wavelength range $5500 - 9000 \text{ \AA}$ with a resolution $R \sim 30,000$ and $S/N \geq 60$. The derived T_{eff} obtained using color indices ($B - V$) and the empirical calibration of Alonso et al. (1999, 2001) for giant stars are lower than our estimates by 350 K in case of HD 49641 and by 318 K in case of HD 58368. Their lower values are likely due to the fact that the color ($B - V$) is affected by CN and C_2 , making the stars redder and as a result the temperature

derived from this color may be lower (Allen And Barbuy 2006). Estimated $\log g$ obtained by them using Hipparcos parallaxes also differ significantly from our estimates. The chemical abundance estimates of Na, Al, α - and iron-peak elements (O, Na, Mg, Al, Si, Ca, Sc, Ti, V, Cr, Mn, Ni) of Yang et al. are found to be similar to the solar abundances. Overabundances of neutron-capture process elements relative to the Sun are noticed in both the stars. The Y I and Zr I abundances are lower than Ba, La and Eu, but higher than the α - and iron-peak elements. The authors noted a positive correlation between Ba intensity and $[\text{Ba}/\text{Fe}]$ in their sample of stars. For the n-capture elements (Y, Zr, Ba, La), there is an anti-correlation between their $[\text{X}/\text{Fe}]$ and $[\text{Fe}/\text{H}]$. With $[\text{Ba}/\text{Fe}] = 1.13$ and 0.98 respectively for HD 49641 and HD 58368, they have confirmed these objects to be strongly enhanced barium stars.

de Castro et al. (2016): In this work the authors have presented an homogeneous analysis of photospheric abundances based on high-resolution spectroscopy of a sample of 182 barium stars and candidates. HD 49641 and HD 58368 are two members of this extended sample. The methodology employed by these authors to derive the stellar parameters are similar to ours. However, there lies significant differences between ours and their estimates of stellar atmospheric parameters, T_{eff} and surface gravity $\log g$. While de Castro et al’s estimates for temperature and $\log g$ for HD 49641 are 4400 K and 1.5 respectively our estimates are significantly higher with values 4700 K and 3.4 . Their estimates of the abundances of α -elements and iron peak elements are similar to those of field giants with the same metallicity. The observed enrichment in sodium is attributed to the operation of Ne-Na cycle. These two stars are also found to exhibit overabundance of the elements created by the s-process. From the measurements of the mean heavy-element abundance pattern as given by the ratio $[\text{s}/\text{Fe}]$, it was found that the barium stars present several degrees of enrichment. From the measured photospheric abundances of the Ba-peak and the Zr-peak elements, $[\text{s}/\text{Fe}]$ and the $[\text{hs}/\text{ls}]$ ratios (where hs refers to heavy s-process elements and ls refers to light s-process elements) are found to be strongly anticorrelated with the metallicity, and that, the barium stars follow an α -metallicity relation.

A comparison of our estimated elemental abundance ratios with their counterparts in Yang et al. (2016) and de Castro et al. (2016) is presented in later sections.

3 HIGH RESOLUTION SPECTRA OF THE SAMPLE STARS

High resolution spectra ($R \sim 42000$) of the four objects selected from the Barium Star Catalogue (Lü 1991) are taken from the ELODIE archive (Moultaka et al. (2004)). The echelle spectrograph ELODIE (Baranne et al. 1996) is attached to the 1.93-m telescope of the Observatoire de Haute Provence (OHP). The spectra cover a wavelength range from 4000 to 6800 \AA . The S/N ratios of these spectra are in the range 109 to 149 at 5500 \AA . An online reduction software TACOS automatically performs an optimal extraction and wavelength calibration of the data. A spectrum is recorded in a single exposure on a 1K CCD that has 67 orders. The

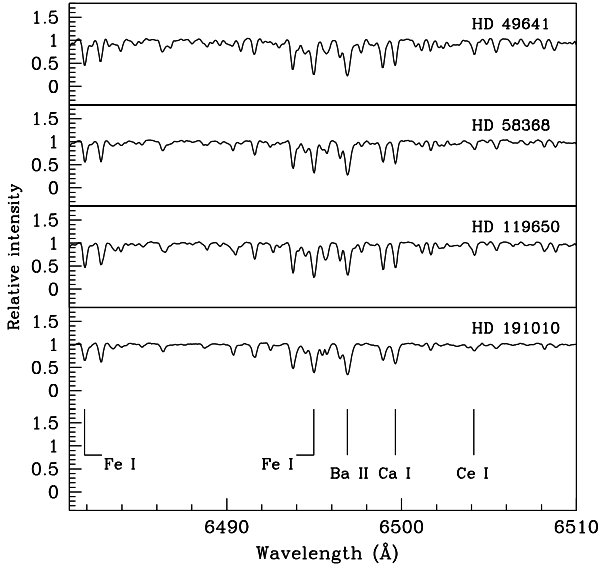


Figure 1. Sample spectra of a few programme stars in the wavelength region 6480 to 6510 Å.

basic data for these objects are listed in Table 1. A few sample spectra are shown in figure 1.

3.1 Photometric temperatures

Photometric temperatures for the objects presented in Table 2 are estimated using the colour temperature calibrations from Alonso et al. (1999) (i.e., equations 4, 9, 10, 11 in Table 2) with its erratum in Alonso et al. (2001). Necessary transformations between the different photometric systems, i.e., from Ramirez and Melendez (2004) and Alonso et al. (1996, 1999) are used to account for the difference between 2MASS infrared photometric system and photometry data measured on the TCS system used in Alonso et al. calibrations.

3.2 Radial velocity

A set of clean unblended lines from each of the object spectrum was selected to estimate the radial velocities. The estimated mean radial velocities are presented in Table 3 along with the literature values for a comparison. The objects show significant variations in radial velocities.

4 STELLAR ATMOSPHERIC PARAMETERS

A selected set of unblended Fe I and Fe II lines (Table 4) with excitation potential in the range 0.0 - 5.0 eV and equivalent width of 20 to 190 mÅ is considered for the determination of the stellar parameters. We have assumed local thermodynamic equilibrium (LTE) for the analysis. An updated 2014 version of MOOG (Snedden 1973) was used for the calculations. The model atmospheres were taken from the Kurucz grid of model atmospheres with no convective overshooting. Solar abundances of the elements are adopted from Asplund, Grevesse & Sauval (2009).

The microturbulent velocity was determined at a given

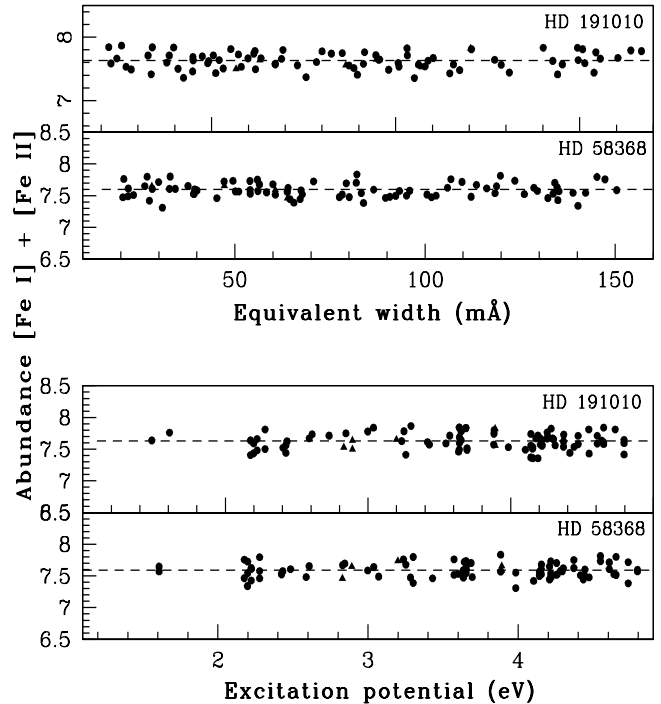


Figure 2. The iron abundances of stars are shown for individual Fe I and Fe II lines as a function of excitation potential in the lower panel. Similarly the iron abundances of stars are shown for individual Fe I and Fe II lines as a function of equivalent width in the upper panel. The abundances correspond to the adopted atmospheric parameters of the stars. The solid circles indicate Fe I lines and solid triangles indicate Fe II lines.

effective temperature by forcing that there be no dependence of the abundances determined using Fe I lines on the equivalent width of the corresponding lines. The effective temperature was determined by making the slope of the abundance versus the excitation potential of Fe I lines to be nearly zero. The initial value of the temperature was taken from the photometric estimates, and a final value arrived at by an iterative method. A few examples for the observed abundances of Fe I and Fe II as a function of excitation potentials and equivalent widths are shown in figure 2. The surface gravity was fixed at a value that gives the same abundances for Fe I and Fe II lines. Clean Fe II lines are more difficult to find than Fe I lines. In most cases, we were limited to 4 - 10 Fe II lines for our analyses. Derived atmospheric parameters are listed in Table 5.

5 ERROR ANALYSIS

The errors in the elemental abundances are mainly due to the errors in deriving the atmospheric parameters which have contributions from the measurement of the equivalent widths of Fe lines. The minimum error in the elemental abundances are taken as the standard deviation of the Fe abundance derived for each objects. These are listed in Tables 6 and 7. The minimum error in temperature is taken as ± 100 K and for $\log g$ as ± 0.1 dex. We have calculated the

Table 1: Basic data for the programme stars

Star ID	RA(2000)	Dec.(2000)	B	V	J	H	K
HD 49641	06 49 29.4495	+03 41 30.189	8.47	7.12	5.078	4.506	4.253
HD 58368	07 25 38.9681	+07 33 39.046	9.01	7.99	6.334	5.919	5.773
HD 119650	13 44 27.1157	+00 42 07.020	8.78	7.59	5.668	5.164	4.908
HD 191010	20 06 45.8410	+25 41 06.790	9.13	8.17	6.488	6.092	5.970

Table 2: Temperatures from photometry

Star Name	T_{eff} (J-K)	T_{eff} (-0.5) (J-H)	T_{eff} (-0.5) (V-K)	T_{eff} (-1.0) (J-H)	T_{eff} (-1.0) (V-K)	T_{eff} (-1.5) (J-H)	T_{eff} (-1.5) (V-K)	T_{eff} (-0.5) (B-V)	T_{eff} (-1.0) (B-V)	T_{eff} (-1.5) (B-V)	Spectroscopic estimates
HD49641	4199	4526	4312	4544	4298	4534	4291	3919	3686	3497	4700
HD58368	4918	5135	4863	5163	4851	5154	4846	4433	4167	3953	5095
HD119650	4350	4779	4445	4802	4432	4792	4425	4152	3904	3703	4825
HD191010	5068	5219	4881	5248	4869	5240	4864	4541	4268	4049	5325

The numbers in the parenthesis below T_{eff} indicate the metallicity values at which the temperatures are calculated. Temperatures are given in Kelvin

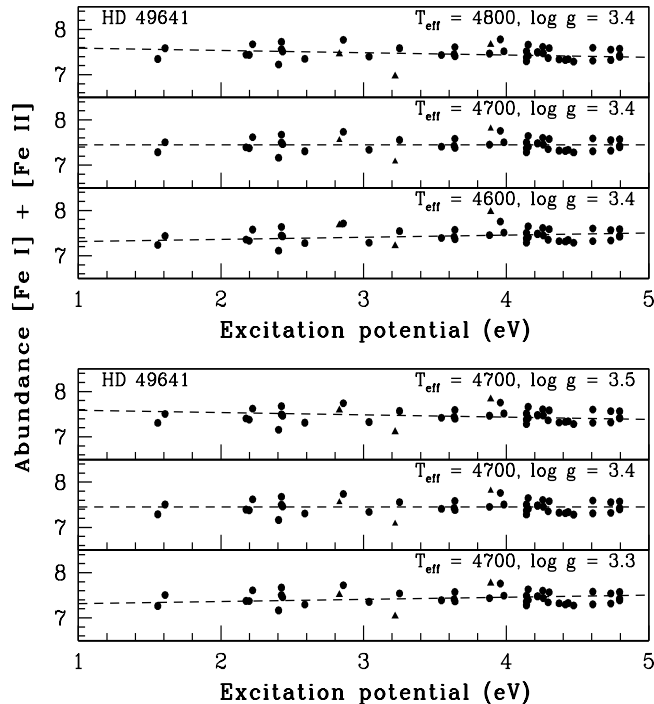


Figure 3. The iron abundances of stars are shown for individual Fe I and Fe II lines as a function of excitation potential. The solid circles indicate Fe I lines and solid triangles indicate Fe II lines. In the upper panel the middle plot shows the abundances corresponding to the adopted T_{eff} . In the same panel the upper and the lower plots show the variation in the abundance trend due to the variation of T_{eff} by + 100 K and - 100 K respectively. In the lower panel the middle plot shows the abundances corresponding to the adopted $\log g$. In the same panel the upper and the lower plots show the variation in the abundance trend due to the variation of $\log g$ by + 0.1 and -0.1 respectively.

errors in the atmospheric parameters as described by Ryan et al. (1996).

In order to show the effect of temperature variations in the abundance pattern we have plotted the Fe abundances with respect to the excitation potential values at three different temperature values, the adopted temperature (T_{eff})

and $T_{eff} \pm 100$ K (figure 3, upper panel). Similarly, the effect on abundance trends due to variation in the adopted $\log g$ values by ± 0.1 dex is also shown in figure 3 (lower panel). The errors presented in tables 6 and 7 correspond to the standard errors when abundances are measured using more than one line. For abundances that are derived using a single line or by using spectrum synthesis calculations an error of ± 0.2 dex is considered. A change by an amount ± 0.2 dex from the adopted abundance is found to be necessary to notice a visual separation between the different synthesized plots.

6 ABUNDANCE ANALYSIS

Elemental abundances are calculated from the measured equivalent widths of lines due to neutral and ionized elements using the 2014 version of MOOG (Snedden 1973) and the adopted model atmospheres. From a close comparison of the spectra of the programme stars with that of the spectrum of Arcturus a line list of all the elements was generated. However, only the lines that were used for abundance analysis are included in the line list; others being blended with contributions from other species could not be used for abundance analysis. The primary source of the adopted $\log gf$ values for the atomic lines due to these elements is Kurucz atomic line database (Kurucz 1995a, b); other sources from literature, such as, Karinkuzhi & Goswami (2014, 2015), Goswami & Aoki (2010), Aoki et al. (2005, 2007), Goswami et al. (2006, 2016), Jonsell et al. (2006), Sneden et al. (1996), Luck and Bond (1991) were also consulted. For the elements Sc, V, Mn, Ba, La and Eu, spectrum synthesis calculation considering hyperfine structure is used to find the abundances. The line list for each region synthesised is taken from Kurucz atomic line list (<http://www.cfa.harvard.edu/amdata/ampdata/kurucz23/sekur.html>). For a few La lines the $\log gf$ values are taken from Lawler et al. (2001).

We had also estimated the Fe abundances considering our line list (Table 4) and using stellar atmospheric models corresponding to the stellar parameters of Yang et al. (2016) for the two objects HD 49641 and HD 58368. In either case we did not arrive at the desired zero slope for ‘abundance vs excitation potential’ plot and ‘abundance vs equivalent width’ plot. We have therefore adopted the stellar param-

Table 3. Radial Velocities of programme stars

Object	V_r km s ⁻¹ (our estimates)	S/N of our spectra at 5500 Å	Date of Observation	V_r km s ⁻¹ (literature values)	References
HD49641	7.20	121	17.12.2000	4.45	1
HD58368	41.67	109	26.11.2001	37.81	1
HD119650	-5.10	143	23.5.2003	-5.70	2
HD191010	20.60	149	29.7.2003	18.10	2

1. Pourbaix et al. (2004); 2. Gontcharov (2006)

Table 4: Equivalent widths (in mÅ) of Fe lines used for deriving atmospheric parameters.

Wavelength (Å)	id	E_{low} (eV)	log gf	HD 49641	HD 58368	HD 119650	HD 191010	References
4348.937	Fe I	2.990	-2.13	–	–	103.9(7.50)	–	1
4551.649		3.943	-2.06	–	–	47.8(7.30)	–	1
4566.514		3.301	-2.25	–	65.5(7.39)	–	–	1
4587.716		3.984	-2.15	–	30.9(7.31)	–	–	1
4602.000		1.608	-3.15	–	118.8(7.65)	129.2(7.38)	–	1
4625.044		3.241	-1.34	–	–	–	–	1
4741.529		2.831	-2.00	–	113.5(7.67)	122.8(7.48)	–	1
4745.800		3.654	-0.79	–	134.7(7.63)	–	–	1
4787.827		2.998	-2.77	–	67.4(7.59)	–	80.0(7.78)	2
4788.751		3.236	-1.81	–	106.8(7.76)	–	108.8(7.63)	1

The numbers in the paranthesis in columns 5-8 give the derived abundances from the respective line.

. References: 1. Führt et al. (1988) 2. Kurucz (1988)

Note: This table is available in its entirety in online only. A portion is shown here for guidance regarding its form and content.

ters estimated by us in determining the abundances of the elements presented in Tables 6 and 7. Derived abundance values along with the abundance ratios with respect to iron are listed in Tables 6 and 7. Lines used for the abundance calculation of these elements are listed in Table 8.

To examine the accuracy of our estimates we have also measured on solar spectra the equivalent widths for a large number of lines (these lines are also detected in the spectra of our programme stars) and measured the solar abundances using the log gf values that we have adopted. The solar atmospheric parameters used are microturbulent velocity 1.25 km s⁻¹, $T_{eff} = 5835$ K and $\log g = 4.55$ cm s⁻². When comparing with Asplund et al. (2009), the derived abundances are found to match closely within a range of 0.08 – 0.1 dex. A comparison of our estimated abundance ratios for elements Na to Zn with respect to Fe, with their counterparts in normal giants and barium stars obtained from literature are shown in figure 4. In figure 5, we have illustrated a few examples of spectrum synthesis calculations for Y, Ba and La. In Table 9, we have presented [ls/Fe], [hs/Fe] and [hs/ls] values, where ls represents the light s-process elements Sr, Y and Zr and hs represents the heavy s-process elements Ba, La, Ce, Nd and Sm. A comparison of our estimated abundance ratios for neutron-capture elements with their counterparts in normal giants and barium stars obtained from literature are shown in figure 6.

6.1 Na and Al

We have derived the Na abundance for all the programme stars using the lines at 5682.65 Å and 5688.22 Å whenever available. The object HD 191010 shows a marginally higher abundance ratio with $[Na/Fe] = 0.59$ than those observed in normal giants (figure 4, upper panel). Many barium stars

studied by de Castro et al. (2016) also show sodium abundance ratios $[Na/Fe]$ in the range 0.3 to 0.6. Sodium does not show any trend with metallicities in field giants. Two of our objects HD 58368 and HD 119650 show sodium abundances similar to many field giants with $[Na/Fe]$ values 0.22, and 0.24 respectively. The object HD 49641 however shows a mild underabundance with $[Na/Fe] = -0.19$ which is somewhat similar to that obtained for the object HD 203137 ($[Na/Fe] = -0.14$) as reported by Yang et al. (2016).

We could not estimate Al abundance as no clear Al lines could be detected due to line blending.

6.2 Mg, Si, Ca, Sc, Ti, V

α -elements in field giants are known to show a slight increase with decreasing metallicity. Three stars in our sample (tables 6 and 7) exhibit abundance ratios of Mg, and Ca lower than that generally seen in normal giants. Our estimated values are however well within the range normally seen in barium stars. This is not surprising as some barium stars are known to exhibit underabundance (Yang et al.(2016) estimated a ratio of $[Mg/Fe] \sim -0.28$ for the two barium stars HD 31308 and HD 224276). While HD 191010 is found to show a near solar value our estimates for the other three objects are -0.41 , -0.39 and -0.16 respectively for HD 49641, HD 58368 and HD 119650. Yang et al. (2016) and de Castro et al. (2016) estimated $[Mg/Fe] = -0.13$ and -0.03 respectively for HD 58368. Abundance ratios of Ti with respect to iron are similar to those generally observed in normal giants and barium stars.

In all the four stars Si abundance is found to be lower than what is normally observed in barium stars and normal giants. Further studies including theoretical aspects would be worthwhile to understand these anomalies.

Table 5: Derived atmospheric parameters for the programme stars.

Star ID	T_{eff} (K)	log g	ζ (km s ⁻¹)	[Fe I/H]	[Fe II/H]
HD 49641	4700	3.40	1.77	-0.05	-0.02
HD 58368	5095	3.45	1.37	0.09	0.12
HD 119650	4825	2.85	1.62	0.04	0.14
HD 191010	5325	2.38	1.92	0.13	0.12

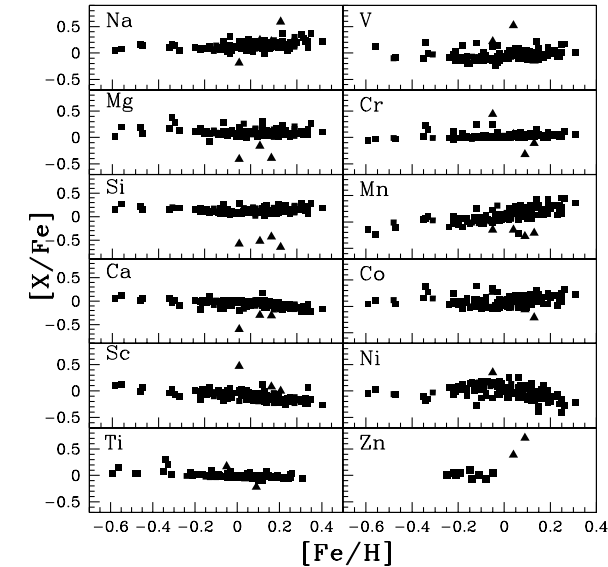
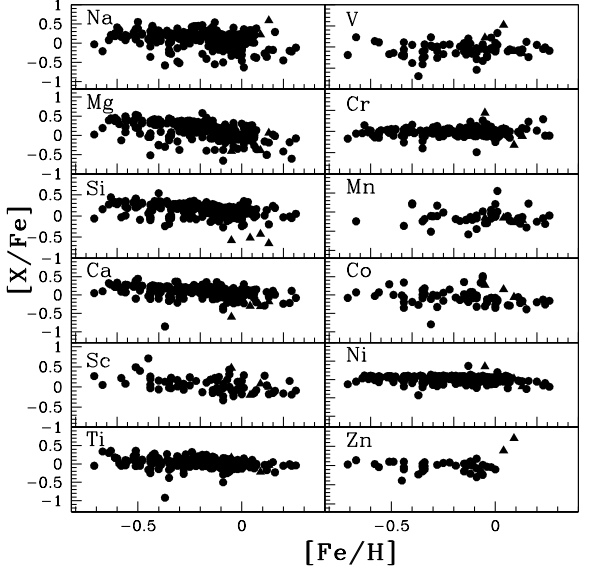


Figure 4. Abundance ratios of light elements observed in the programme stars with respect to $[Fe/H]$. In the upper panel our programme stars (solid triangles) are compared with the abundance ratios observed in Ba stars (solid circles) from literature (i.e., Allen & Barbuy (2006), Liang et al. (2003), Smiljanic et al. (2007), Zacs (1994), de Castro et al. 2016)). In the lower panel our program stars (solid triangles) are compared with the abundance ratios observed in giants (solid squares) from literature (i.e., Luck and Heiter (2007), Mishenina et al. (2006)).

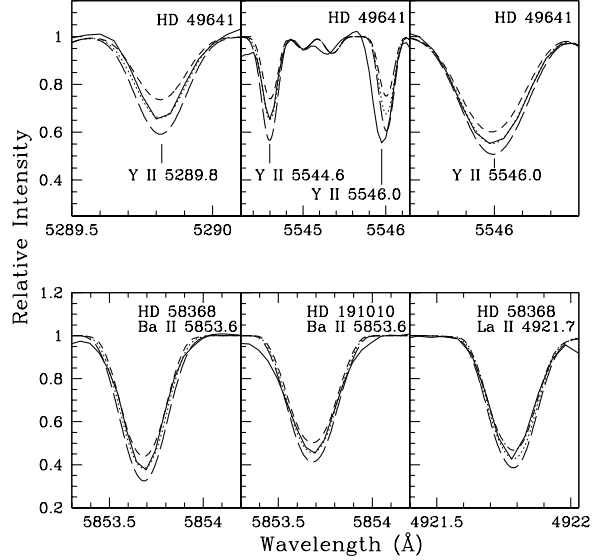


Figure 5. Spectral-synthesis fits of Ba II line at 5853.6 Å and La II line at 4921.7 Å are shown for two objects HD 58368 and HD 191010 in the lower panel. In the upper panel, spectral-synthesis fits of Y II line at 5289.815 Å, 5544.615 Å, and 5546.009 Å, are shown for HD 49641. The dotted lines indicate the synthesized spectra and the solid lines indicate the observed line profiles. Two alternative synthetic spectra at the (adopted value + 0.3, long-dashed line) and (adopted value - 0.3, short-dashed line) are shown to demonstrate the sensitivity of the line strength to the abundances. we could get good fits using the adopted value of the corresponding elements (Tables 6 and 7).

While Sc abundance ratios in three stars are similar to those observed in normal giants, HD 49641 shows a higher value with $[Sc/Fe] = 0.47$. Sc abundance ratios are well within the range seen in barium stars. The abundance ratio of V in HD 119650 is marginally higher ($[V/Fe] = 0.52$) than those seen in normal giants. Although abundance of V is calculated using measured equivalent widths for many lines, this being an odd Z element its abundance is also estimated from spectrum synthesis calculation of V I line at 5727.028 Å taking into account the hyperfine components from Kurucz database. The values obtained from spectrum synthesis calculations are listed in the abundance tables. The Sc abundance is estimated using the Sc II line at 6245.63 Å considering hyperfine structure from Prochaska & McWilliam (2000).

6.3 Cr, Mn, Co, Ni, Zn

Abundance ratios of iron peak elements exhibit similar values as seen in barium stars. However, a close agreement with the values of normal giants are not observed in all the cases. Cr abundances derived using Cr I lines show near solar values for HD 119650 (+0.06) and HD 191010 (−0.11). Cr is overabundant in HD 49641 with $[\text{Cr}/\text{Fe}] = 0.44$ and underabundant in HD 58368 with $[\text{Cr}/\text{Fe}] = -0.32$. Cr abundances measured using Cr II lines whenever possible also give similar results.

Mn abundance is obtained using spectrum synthesis calculation of 6013.51 Å line taking into account the hyperfine structures from Prochaska & McWilliam (2000).

We could estimate Zn abundance only in two stars, HD 58368 and HD 119650 using a single Zn I line at 4722.15 Å. This line returns a value $[\text{Zn}/\text{Fe}] = 0.71$ and 0.39 respectively which are higher than those normally seen in normal giants and barium stars (figure 4).

6.4 Sr, Y, Zr

We have estimated the abundance of Sr using the Sr I line at 4607.327 Å. Sr is overabundant in all the four stars with $[\text{Sr}/\text{Fe}]$ values 0.97, 1.19, 1.01 and 1.36 for HD 49641, HD 58368, HD 119650 and HD 191010 respectively. None of the Sr II lines detected in the spectra are found suitable for abundance estimate.

Among the three light s-process elements Yang et al. (2016) and de Castro et al. (2016) have reported abundances only for Y and Zr. These values for HD 49641 and HD 58368 are respectively (Y: 0.35, 0.41; Zr: 0.41, 0.25; Yang et al.) and (Y: 0.89, 0.85; Zr: 0.53, 0.60; de Castro et al.).

We could measure the abundance of Y in all the four stars. Y is found to be significantly overabundant in HD 49641. We have performed spectrum synthesis calculation for three Y II lines at 5289.815, 5544.615 and 5546.009 for the object HD 49641 (figure 5). An Y abundance of 3.50 gives satisfactory fits for the lines of Y II at 5289.815 and 5544.615 Å giving $[\text{Y}/\text{Fe}] = 1.31$. In Table 6, we have listed this value. The Y II line at 5546.009 Å can be fitted with a slightly higher abundance 4.15 that gives $[\text{Y}/\text{Fe}] = 1.96$. However, this line is blended with a line due to vanadium. Estimated $[\text{Y}/\text{Fe}]$ values are 1.12, 0.68 and 0.11 in HD 58368, HD 119650 and HD 191010 respectively.

We could derive Zr abundance for three objects from Zr I lines. HD 49641 and HD 58368 both show an overabundance with $[\text{Zr}/\text{Fe}] = 0.73$. HD 119650 also show a mild enhancement with a value of $[\text{Zr}/\text{Fe}] = 0.42$. Zr abundance could not be estimated for HD 191010.

6.5 Ba, La, Ce, Pr, Nd, Sm, Eu, Dy

Abundances ratios of these elements with respect to iron are compared with their counterparts observed in normal giants and barium stars in figure 6. We could estimate abundances of these elements in all the stars except for HD 49641 where abundances of Sm and Dy could not be estimated. While de Castro et al (2016) had estimated abundances of only La, Ce and Nd, for HD 49641 and HD 58368, Yang et al. (2016) estimated abundances of only Ba, La, and Eu for these two objects.

As can be seen from Table 12, for a few elements our estimates are significantly different from these two studies. As expected, the two stars with $[\text{Ba}/\text{Fe}] > 1.0$, show abundances for other heavy elements higher values than that generally noticed in normal giants. The object HD 119650 with $[\text{Ba}/\text{Fe}] < 0.52$ show $[\text{X}/\text{Fe}] > 1.0$ for La, Sm and Dy and for the rest of the elements, $[\text{X}/\text{Fe}] < 1.0$. In case of HD 191010 the heavy elements are found to show $[\text{X}/\text{Fe}] < 0.52$. The heavy elements in normal giants and barium stars are known to show large scatter with respect to metallicity.

As many lines due to Ce, Pr, Nd, and Sm could be measured on our spectra, the standard abundance determination method using equivalent width measurements are used for abundance estimates. Spectrum synthesis calculation is performed for Ba, La and Eu. The presented abundance for Ba, La and Eu in the Tables 6 and 7 are from spectrum synthesis calculations and indicated in Table 8.

Ba abundance is derived from spectrum synthesis calculation using Ba II line at 5853.668 Å considering hyperfine components from McWilliam (1998). La abundance for all the stars are derived from spectrum synthesis calculation of La II line at 4921.77 Å considering hyperfine components from Jonsell et al. (2006), and, Eu abundance is determined from spectrum synthesis calculation of Eu II line at 6645.130 Å by considering the hyperfine components from Worley et al. (2013).

6.6 Stellar Masses

We have derived the masses of the programme stars from their locations in the Hertzsprung-Russel diagram, using the Girardi et al. (2000) database of evolutionary tracks and our estimates of $\log(L/L_\odot)$ and T_{eff} (figure 7). While $\log(L/L_\odot)$ is derived by photometric methods using the parallax values from the Hipparcos catalogue (van Leeuwen 2007); for T_{eff} we have used our spectroscopic estimates. We have selected evolutionary tracks with initial compositions, $Z = 0.019$ and $Y = 0.273$, where Z is initial metallicity and Y is initial helium abundance. The approximated masses derived for the programme stars are presented in Table 10. It is to be noted that these mass estimates are only indicative as the Hipparcos parallaxes for these four objects have large uncertainty in measurements that amounts to ~ 35 to 43 % for three stars and the largest uncertainty showing for HD 119650 with $\sim 75\%$.

7 PARAMETRIC MODEL BASED STUDY

We have examined the origin of the neutron-capture elements by comparing the observed abundances with the predicted s- and r- process contribution using appropriate model function in the framework of a parametric model.

We have utilized the solar system r- and s- process isotopic abundances of stellar models offered by Arlandini et al. (1999). The observed elemental abundances are scaled to the metallicity of the corresponding stars and normalized to their respective barium abundances. Elemental abundances are then fitted with the parametric model function $\log \epsilon_i = A_s N_{is} + A_r N_{ir}$

where N_{is} indicates the abundance from s-process, N_{ir} indicates the abundance from r-process; A_s indicates the

Table 6 : Elemental abundances in HD 49641 and HD 58368

		HD 49641				HD 58368		
Z		solar $\log\epsilon^a$	$\log\epsilon$	[X/H]	[X/Fe]	$\log\epsilon$	[X/H]	[X/Fe]
Na I	11	6.24	6.00±0.20	-0.24	-0.19	6.55±0.15	+0.31	+0.22
Mg I	12	7.60	7.14±0.07	-0.46	-0.41	7.39±0.11	-0.30	-0.39
Si I	14	7.51	6.88±0.06	-0.63	-0.58	7.17±0.19	-0.34	-0.43
Ca I	20	6.34	5.69±0.20	-0.65	-0.60	6.12±0.12	-0.22	-0.31
Sc II	21	3.15	3.70±.20	+0.45	+0.47	3.35±0.20	+0.20	+0.08
Ti I	22	4.95	5.07±0.14	+0.12	+0.17	4.82±0.16	-0.13	-0.22
Ti II	22	4.95	-	-	-	5.08±0.01	+0.13	+0.04
V I	23	3.93	4.10±0.20	0.17	0.22	3.92±0.20	-0.01	-0.10
Cr I	24	5.64	6.03±0.18	+0.39	+0.44	5.41±0.11	-0.23	-0.32
Mn I	25	5.43	5.23±0.20	-0.20	-0.15	5.25±0.20	-0.18	-0.27
Fe I	26	7.50	7.45±0.13	-0.05	-	7.59±0.12	+0.09	-
Fe II	26	7.50	7.48±0.30	-0.02	-	7.62±0.110	+0.12	-
Co I	27	4.99	5.21±0.13	+0.22	+0.27	5.04 ±0.17	+0.05	-0.06
Ni I	28	6.22	6.52±0.18	+0.30	+0.35	6.33±0.13	+0.11	+0.02
Sr I	38	2.87	3.79±0.20	+0.92	+0.97	4.15±0.20	+1.28	+1.19
Y II	39	2.21	3.50±0.20	+1.29	+1.31	3.45±0.04	+1.24	+1.12
Zr I	40	2.58	3.29 ±0.20	+0.71	+0.73	3.40±0.07	+0.82	+0.73
Ba II	56	2.18	3.32±0.20	+1.14	+1.16	3.50±0.20	+1.32	+1.20
La II	57	1.10	2.60±0.20	+1.50	+1.52	2.70±0.20	+1.60	+1.48
Ce II	58	1.58	3.24±0.04	+1.66	+1.68	2.97±0.07	+1.39	+1.27
Pr II	59	0.72	2.42±0.08	+1.70	+1.72	1.83±0.12	+1.11	+0.99
Nd II	60	1.42	3.00±0.12	+1.58	+1.60	2.47±0.17	+1.05	+0.93
Sm II	62	0.96	-	-	-	2.09±0.20	+1.13	+1.01
Eu II	63	0.52	1.40±0.20	+0.88	+0.90	0.99±0.20	+0.57	+0.45
Dy II	66	1.10	-	-	-	3.17±0.20	+2.07	+1.95

^a Asplund et al. (2009)

Table 7: Elemental abundances in HD 119650 and HD 191010

		HD 119650				HD 191010		
Z		solar $\log\epsilon^a$	$\log\epsilon$	[X/H]	[X/Fe]	$\log\epsilon$	[X/H]	[X/Fe]
Na I	11	6.24	6.52±0.30	+0.28	+0.24	6.96±0.20	+0.72	0.59
Mg I	12	7.60	7.48±0.07	-0.12	-0.16	7.79±0.08	+0.19	+0.06
Si I	14	7.51	7.03±0.17	-0.48	-0.52	6.99±0.20	-0.52	-0.65
Ca I	20	6.34	6.08±0.19	-0.26	-0.30	6.29±0.12	-0.05	-0.18
Sc II	21	3.15	3.25±0.20	-0.10	-0.20	3.27±0.20	+0.12	0.00
Ti I	22	4.95	4.97±0.17	-0.02	-0.06	4.85±0.15	0.10	-0.03
Ti II	22	4.95	5.12±0.18	+0.17	+0.07	5.30±0.07	+0.35	+0.23
V I	23	3.93	4.49±0.20	+0.56	+0.52	3.95±0.20	-0.02	-0.15
Cr I	24	5.64	5.74±0.21	+0.10	+0.06	5.66±0.19	+0.02	-0.11
Mn I	25	5.43	5.32±0.11	-0.11	-0.15	5.25±0.20	-0.18	-0.21
Fe I	26	7.50	7.54±0.20	+0.04	-	7.63±0.13	+0.13	-
Fe II	26	7.50	7.60±0.20	+0.10	-	7.62±0.12	+0.12	-
Co I	27	4.99	5.18±0.16	+0.19	+0.15	4.91±0.15	-0.08	-0.21
Ni I	28	6.22	6.21±0.13	-0.01	-0.05	6.16±0.14	-0.06	-0.19
Zn I	30	4.56	4.99±0.20	+0.43	+0.39	-	-	-
Sr I	38	2.87	3.92±0.20	+1.05	+1.01	4.36 ±0.20	+1.49	+1.36
Y II	39	2.21	2.99±0.18	+0.78	+0.68	2.54 ±0.15	+0.23	+0.11
Zr I	40	2.58	3.04±0.20	+0.46	+0.42	-	-	-
Ba II	56	2.18	2.80±0.20	+0.62	+0.52	2.70 ±0.20	+0.52	+0.40
La II	57	1.10	2.20±0.20	+1.10	+1.00	1.64±0.20	+0.54	+0.42
Ce II	58	1.58	2.35±0.10	+0.77	+0.67	2.16±0.06	+0.58	+0.46
Pr II	59	0.72	1.41±0.20	+0.69	+0.59	1.40±0.20	+0.68	+0.52
Nd II	60	1.42	1.92±0.09	+0.50	+0.40	1.66±0.09	+0.24	+0.12
Sm II	62	0.96	2.35±0.13	+1.39	+1.29	0.90±0.20	-0.06	-0.18
Eu II	63	0.52	1.00±0.20	+0.48	+0.38	0.72±0.20	+0.20	+0.08
Dy II	66	1.10	2.74±0.09	+1.64	+1.54	2.31±0.20	+1.21	+1.09

^a Asplund et al. (2009)

Table 8: Equivalent widths (in mÅ) of lines used for calculation of elemental abundances.

Wavelength (Å)	Id	E_{low} (eV)	log gf	HD 49641	HD 58368	HD 119650	HD 191010	references
5682.650	Na I	2.100	-0.70	–	143.4(6.66)	158.1(6.72)	–	1
5688.220		2.100	-0.40	150.6(6.00)	150.6(6.44)	154.1(6.32)	178.1(6.96)	2
5889.950		0.000	0.10	847.9(5.60)	746.8(6.06)	913.1(6.12)	577.3(6.42)	3
5895.920		0.000	-0.20	567.7(5.50)	507.4(6.00)	610.6(6.03)	470.8(6.49)	3
4702.990	Mg I	4.350	-0.67	228.1(7.19)	219.2(7.46)	227.6(7.53)	215.6(7.85)	4
5528.400		4.350	-0.49	237.1(7.09)	218.2(7.30)	239.9(7.43)	227.3(7.73)	4
5711.088		4.346	-1.83	–	–	138.7(7.69)	–	4
4947.607	Si I	5.082	-1.82	19.0(6.92)	24.4(7.02)	22.2(6.87)	28.5(6.99)	2
5666.677		5.616	-1.05	22.2(6.83)	–	36.5(7.00)	–	2
6138.515		5.984	-1.35	–	–	–	44.7(7.68)	2

The numbers in the paranthesis in columns 5-8 give the derived abundances from the respective line.

References: 1. Kurucz (1988), 2. Kurucz & Peytremann (1975), 3. Wiese et al. (1966), 4. Martin et al. (1988a)

Note: This table is available in its entirety in online only. A portion is shown here for guidance regarding its form and content.

Table 9: Observed values for [Fe/H], [ls/Fe], [hs/Fe] and [hs/ls]

Star Name	[Fe/H]	[ls/Fe]	[hs/Fe]	[hs/ls]
HD 49641	-0.05	1.33	1.49	0.16
HD 58368	0.09	1.01	1.18	0.17
HD 119650	0.04	0.70	0.78	0.08
HD 191010	0.13	0.74	0.24	-0.50

component coefficient that correspond to contributions from the s-process and A_r indicates the component coefficient that correspond to contributions from the r-process. The best fit coefficients and reduced chi-square values for the programme stars are given in Table 11. While in the case of HD 49641 the observed abundances of neutron-capture elements seem to have similar contribution from s- and r-process, for the objects HD 58368 and HD 191010 contributions from s-process seem to dominate. HD 119650 seem to have more contributions from r-process; this object also shows Sm and Dy with values $[X/Fe] > 1.0$.

8 CONCLUSIONS

Elemental abundances are presented for four peculiar stars listed in the Barium star catalogue of Lü (1991). All the objects are found to be low-velocity objects ($V_r < 45$ km/s). Except for HD 119650 the estimated radial velocities for these objects are significantly different from the previous estimates (Table 3). Metallicity estimates indicate that they are mostly solar or near-solar objects, with metallicity $[Fe/H]$ ranging from -0.03 to $+0.1$ dex. Barium is enhanced in HD 49641 and HD 58368 with $[Ba/Fe] > 1.0$; the other two objects, HD 119650 and HD 191010 are found to be mild barium stars with $[Ba/Fe] \sim 0.52$ and 0.4 respectively. These two later objects show large enhancement of Sr, with $[Sr/Fe] = 1.01$ and 1.36 respectively.

A comparison of the abundance ratios of the heavy elements with those available in literature, including the large sample of de Castro et al. (2016) (for Y, Zr, La, Ce and Nd) show that the abundance ratios of the programme stars are well within the range generally noticed in barium stars (figure 6).

Anomalies in abundance ratios of α -elements are noticed in a few objects. Sc, V and Mn in the program stars show similar values as seen in other barium stars. In two

objects HD 58368 and HD 119650, Zn shows clearly higher values than what is generally noticed in barium stars as well as in normal giants. Na, Mg, Si, Sc, V, Cr, and Co show large scatter with respect to metallicity. It is to be noted that the Galactic Chemical Evolution (GCE) model predictions for the evolution of Sc, V, and Ti (figure 7, in Goswami & Prantzos (2000)) show trends that are similar to the observed trends of these elements. This implies that the origin of these elements are likely from massive stars. The behavior of Sc is also compatible with the results of Nissen et al. (2000), Chen et al. (2000a) and Goswami and Prantzos (2000), who demonstrated that $[Sc/Fe]$ decreases with increasing metallicity in disk stars.

The estimated masses are $2.5M_{\odot}$, $2.3M_{\odot}$, $2.5M_{\odot}$ and $3.0M_{\odot}$ for HD 49641, HD 58368, HD 119650 and HD 191010 respectively. The mass of HD 58368 is within the average mass of typical mild Ba stars, i.e., 1.9 or $2.3M_{\odot}$ with the 0.60 or $0.67 M_{\odot}$ companion white dwarfs Jorissen et al.(1998).

It has been argued that a metallicity lower than solar is required to form a barium star. The increasing levels of heavy-element overabundances observed in the sequence of mild to barium-strong stars support that hypothesis. Kovacs (1985) also noticed that there is a correlation between $[Ba/Fe]$ and metallicity $[Fe/H]$: strong barium stars generally have a metallicity lower than mild barium stars. The estimated metallicity of HD 49641 ($[Fe/H] = -0.03$, $[Ba/Fe] = 1.16$), HD 58368 ($[Fe/H] = 0.1$, $[Ba/Fe] = 1.20$), HD 119650 ($[Fe/H] = 0.07$, $[Ba/Fe] = 0.52$), HD 191010 ($[Fe/H] = 0.12$, $[Ba/Fe] = 0.40$) do not exactly show this trend.

The object HD 49641 clearly shows the characteristics of a barium star with the heavy elements Ba, La, Ce, Pr and Nd showing a value $[X/Fe] > 1$, Another interesting feature of this object is its high abundance of Y with $[Y/Fe] = 1.31$. With many heavy elements significantly enhanced together with the variations observed in radial velocity estimates a mass-transfer scenario similar to the ones that hold for barium stars, CH stars and CEMP-s stars is likely for

Table 10: **Derived Masses (M_{\odot}) of programme stars**

Object	$\log(L/L_{\odot})$	$\log(T_{eff})$	Mass(in M_{\odot})
HD 49641	2.04	3.67	2.5
HD 58368	1.50	3.70	2.3
HD 119650	1.93	3.68	2.5
HD 191010	1.96	3.73	3.0

Table 11: **Best fit coefficients and reduced chi-square values**

Star Name	A_s	A_r	χ^2
HD 49641	0.56 ± 0.10	0.59 ± 0.09	1.71
HD 58368	0.67 ± 0.08	0.25 ± 0.08	0.76
HD 119650	0.39 ± 0.08	0.63 ± 0.07	0.80
HD 191010	0.80 ± 0.08	0.21 ± 0.08	0.95

the origin of this object. However, Europium is also found to be enhanced in this object with $[Eu/Fe] = 0.90$. Such an enhancement of Eu can not be explained based on only binary pictures. Further investigation of its formation scenario is necessary to understand its abundance patterns.

The object HD 58368 is a barium star with $[Ba/Fe] = 1.20$. Light *s*-process elements Sr, Y and Zr show large enhancement with $[Sr/Fe] = 1.2$, $[Y/Fe] = 1.12$ and $[Zr/Fe] = 0.73$. Eu shows a mild enhancement with $[Eu/Fe] = 0.45$. McClure (1983) found this object to be a radial velocity variable with a variation of $\sim \pm 12 \text{ Km s}^{-1}$ indicating its binarity. A mass-transfer scenario is likely to hold for this object too. The other two objects HD 119650, HD 191010 show mild enhancement in barium. While La is enhanced in HD 119650 with $[La/Fe] = 1.0$, this element is mildly enhanced in HD 191010 with $[La/Fe] = 0.42$. Similarly Sm is highly abundant in HD 119650 with $[Sm/Fe] = 1.3$ and underabundant in HD 191010 with $[Sm/Fe] = -0.18$. Eu is only mildly enhanced in HD 119650 with $[Eu/Fe] = 0.38$ and exhibits a near-solar value in HD 191010 with $[Eu/Fe] = +0.08$. Other elements Ce, Pr and Nd are enhanced but not >1.0 with respect to Fe. A mass-transfer scenario suggested for barium stars might have operated in these two objects.

Acknowledgements

We are grateful to an anonymous referee for many constructive suggestions which have improved considerably the readability of the paper. This work made use of the SIMBAD astronomical data base, operated at CDS, Strasbourg, France, and the NASA ADS, USA. We would like to acknowledge Sreejith P Babu for performing some initial calculations during his internship at IIA, Jan - May, 2014. Funding from the DST project SB/S2/HEP-010/2013 is gratefully acknowledged.

REFERENCES

Allen, D.M., Barbuy, B. 2006a, *A&A*, 454, 895
Alonso A., Arribas S., Martinez-Roger C., 1996 *A&A*, 313, 873
Alonso A., Arribas S. & Martinez-Roger C., 1999, *A&AS*, 140, 261
Aoki W. et al., 2005, *ApJ*, 632, 611
Aoki, W., Beers, T. C., Christlieb N., Norris, J. E., Ryan, S. G., Tsangarides, S. 2007, *ApJ*, 655, 492

Arlandini et. al., 1999, *ApJ*, 525, 886
Arnesen A., Bengtsson A., Hallin R., Lindskog J., Nordling C., and Noreland T. 1977, *Phys.Scripta* 16, 31-34.
Asplund M., Grevesse N., Sauval A. J., 2009, *Ann. Rev. Astron. Astrophys.*, 47:481
Baranne A., Queloz D., Mayor M., Adranzyk G., Knispel G., Kohler D., Lacroix D., Meunier J. P., Rimbaud G., Vin A., 1996, *A&AS*, 119, 373
Bidelman, W. P. & Keenan, P. C., 1951, *ApJ*, 114, 473
Biemont E., Grevesse N., Hannaford p., Lowe R. M., 1981, *ApJ*, 248, 867
Biemont E., Karner C., Meyer G., Traeger F., and zu Putlitz G. 1982, *A&A* 107, 166-171.
Boffin, H. M. J., & Jorissen, A. 1988, *A&A*, 205, 155
Chen, Y. Q., Nissen, P. E., Zhao, G., et al. 2000a, in *The Galactic Halo: From Globular Cluster to Field Stars*, Proceedings of the 35th Liege International Astrophysics Colloquium, eds., A. Noels, P. Magain, D. Caro, et al., Belgium: Institut d'Astrophysique et de Geophysique, 35, 219
Corliss C.H. and Bozman W.R. 1962a, *NBS Monograph* 53.
Corliss C.H. and Bozman W.R. 1962b, *NBS Monograph* 53, adjusted
Cowley, C.R. and Corliss, C.H. 1983, *MNRAS* 203, 651
de Castor, D. B., Pereira, C. B., Roig F., Jilinski E., Drake N. A., Chavero, C., Sales Silva J. V., 2016, *MNRAS*, 459, 4299
Elias, J. H., Gregory, B., Phillips, M. N., Williams, R.E., Graham, J. R., Meikle, W.P.S., Schwartz, K. D., and Wilking, B., 1988, *ApJ*, 331, L9
Führ J. R., Martin G. A., Wiese W. L., 1988, *J. Phys. Chem. Ref. Data*, 17, 4
Girardi L., Bressan A., Bertelli G., Chiosi C., 2000, *A&AS* 141, 371
Gontcharov G.A., 2006, *AstL*, 32, 759
Goswami A., Prantzos N., 2000, *A&A*, 359, 191
Goswami A., Aoki W., Beers T. C., Christlieb N., Norris J., Ryan S. G., Tsangarides S. 2006, *MNRAS*, 372, 343
Goswami A., & Aoki W., 2010, *MNRAS*, 404, 253
Goswami A., & Aoki W., Karinkuzhi D., 2016, *MNRAS*, 455, 402
Han, Z., Eggleton, P. P., Podsiadlowski, P., & Tout, C. A. 1995, *MNRAS*, 277, 1443
Hannaford P., Lowe R.M., Grevesse N., Biemont E., and Whaling W 1982, *ApJ* 261, 736-746.
Izzard, R. G., Dermine, T. & Church, R. P. 2010, *A&A*, 523, 10
Ji Alexander P., Frebel A., Simon Jashua D., Geha M., 2015, (arxiv:1510.07632)
Jonsell K., Barklem P. S., Gustafsson B., Christlieb N., Hill V., Beers T. C., & Holmberg J., 2006, *A&A*, 451, 651
Jorissen, A., Van Eck S., Mayor M., Udry S., et al., 1998, *A&A*,

Table 12: comparison with literature values

starname	T_{eff}	logg	[Fe/H]	[Na/Fe]	[Mg/Fe]	[Si/Fe]	[Ca/Fe]	[Sc/Fe]	[Ti/Fe]	[V/Fe]	[Cr/Fe]	[Mn/Fe]	[Co/Fe]	[Ni/Fe]	ref
HD49641	4700	3.4	-0.05	-0.19	-0.41	-0.58	-0.60	+0.47	+0.17	+0.22	+0.44	-0.15	+0.27	+0.35	1
	4351	1.05	-0.32	-0.03	0.49	0.40	0.21	0.07	0.04	-0.02	0.17	0.20	-	0.03	2
	4400	1.5	-0.30	+0.24	0.10	0.22	0.07	-	-0.02	-	0.04	-	-	0.05	3
HD58368	5095	3.45	+0.09	+0.22	-0.39	-0.43	-0.31	+0.08	-0.22	-0.10	-0.32	-0.27	-0.06	+0.02	1
	4777	2.47	-0.11	0.24	-0.03	0.27	-0.08	0.09	-0.18	-0.35	-0.04	-0.02	-	0.02	2
	5000	2.6	+0.04	0.11	-0.13	0.12	0.06	-	-0.01	-	-0.04	-	-	0.02	3

1. Our work; 2. Yang et al. (2016); de Castro et al. (2016)

Table 12: continued

starname	[Sr/Fe]	[Y/Fe]	[Zr/Fe]	[Ba/Fe]	[La/Fe]	[Ce/Fe]	[Pr/Fe]	[Nd/Fe]	[Sm/Fe]	[Eu/Fe]	[Dy/Fe]	ref
HD49641	0.97	+2.29	0.73	1.16	1.52	1.68	1.72	1.60	-	+0.90	-	1
	-	0.35	0.45	1.13	1.38	-	-	-	-	0.64	-	2
	-	0.89	0.53	-	1.86	1.04	-	1.14	-	-	-	3
HD58368	1.19	1.12	0.73	1.20	1.48	1.27	0.99	0.93	1.01	0.45	1.95	1
	-	0.14	0.25	0.98	1.07	-	-	-	-	0.41	-	2
	-	0.85	0.60	-	1.13	0.86	-	0.69	-	-	-	3

1. Our work; 2. Yang et al. (2016); 3. de Castro et al. (2016)

- 332, 877
- Karinkuzhi D. & Goswami A., 2014, MNRAS, 400, 1095
- Karinkuzhi D. & Goswami A., 2015, MNRAS, 446, 2348
- Kovacs N., 1985, A&A, 150, 232
- Kurucz, R. L., 1988, ASSL, 138, 41
- Kurucz R. L., 1995a, in ASP Conf. Proc. 78, Astrophysical Applications of Powerful New Databases, ed. S. J. Adelman & W. L. Wiese (San Francisco:ASP), 205
- Kurucz R. L., 1995b, in ASP Conf. Proc. 81, Laboratory and Astronomical High Resolution Spectra, ed. A. J. Sauval, R. Blomme, & N. Grevesse (San Francisco:ASP), 583
- Kurucz, R. L.; Peytreman, E., 1975, SAOSR, 362
- Lage C.S. and Whaling W. 1976, JQSRT 16, 537-542.
- Lawler J. E., BonVallet G., Sneden C., 2001, ApJ, 556, 452
- Liang, Y. C., Zhao, G., Chen, Y. Q., Qiu, H. M., & Zhang, B. 2003, A&A, 397, 257
- Lü Phillip, K. 1991, AJ, 101, 2229
- Luck, R.E., Bond H.E., 1991, ApJS, 77, 515
- Luck R. E., Heiter U., 2007, AJ, 133, 2464
- Martin, G. A., Führ J. R., Wiess, W. L., 1988a, J. Phys. Chem. Ref. data, 17, Suppl. 3
- Martin, G. A., Führ J. R., Wiess, W. L., 1988a, J. Phys. Chem. Ref. data, 17, Suppl. 3 (modified)
- MacConnell, D. J, Frye R. L. & Upgren, A. R., 1972, AJ, 77, 384
- McClure, R. D. 1983, ApJ, 268, 264
- McClure, R. D. 1984, PASP, 96, 117
- McClure, R. D., Fletcher, J. M., & Nemeck, J. 1980, ApJ, 238, L35
- McEachran R.P., and Cohen M. 1971, JQSRT, 11, 1819.
- McWilliam A., 1998, AJ, 115, 1640
- Meggers W.F, Corliss C.H. and Scribner B.F. 1975, NBS Monograph 145. estimated from intensity
- Mennessier, M. O., Luri, X., Figueras, F., Gomez, A. E., Grenier, S., Torra, J., & North, P. 1997, A&A, 326, 722
- Mishenina T. V., Bienaym O., Gorbaneva T. I., Charbonnel C., Soubiran C., Korotin S. A., Kovtyukh, V. V., 2006, A&A, 456, 1109
- Moultaka J., Ilovaisky S. A., Prugniel P., Soubiran C., 2004, PASP, 116, 693
- Nissen, P. E., Chen, Y. Q., Schuster, W. J., & Zhao, G. 2000, A&A, 353, 722
- Prochaska, J. X., & McWilliam A., 2000, ApJ, 537, L57
- Poubirax et al., 2004, A&A, 424, 727
- Ramirez I., Melendez J., 2004, ApJ, 609, 417
- Ryan, S. G., Norris, J. E., Beers, T. C., 1996, ApJ, 471, 254
- Smiljanic, R., Porto de Mello, G. F., & da Silva, L. 2007, A&A, 468, 679
- Sneden C., 1973, PhD thesis, Univ. Texas at Austin
- Sneden C., McWilliam A., Preston G. W., Cowan J.J., Burris D. L., Armosky B. J., 1996, Apj, 467, 819
- Tautvaišienė G., Edvardsson, B., Tuominen, I., Ilyin, I., 2000, A&A, 460, 399
- Udry, S., Jorissen, A., Mayor, M., & Van Eck, S. 1998a, A&AS, 131, 25
- Udry, S., Mayor, M., Van Eck, S., et al. 1998b, A&AS, 131, 43
- Van der Swaelmen, M., Barbuy, B., Hill, V., Zoccali M., Minniti, D., Ortolani, S., and Gómez, A., 2016, A&A, 586, 1
- Van Leeuwen F., 2007, A&A, 474, 653
- Ward L., Vogel O., Arnesen A., Hallin R., and Wannstrom A. 1985a, Phys. Scripta 31, 162
- Ward, L., Vogel, O., Arnesen, A., Hallin, R., and Wannstrom, A. 1985b, Phys. Scripta 31, 162, modified
- Warner, B. 1968, MNRAS 140, 53
- Wiese W.L., Smith M.W., and Glennon B.M. 1966, NSRDS-NBS 4.
- Worley C. C, Hill V., J. Sobeck J., Carretta E., A&A, 2013, 553, A47
- Yang, Guo-Chao, Liang Yan-Chun, Spite M., Chen Yu-Qin, Zhao, G., Zhang Bo, Liu Guo-Qing, Liu Yu-Juan, Liu N., Deng Li-Cai, Spite F., Hill V., Zhang Cai-Xia, 2016, RAA, 16, No.1
- Zacs, L. 1994, A&A, 283, 937

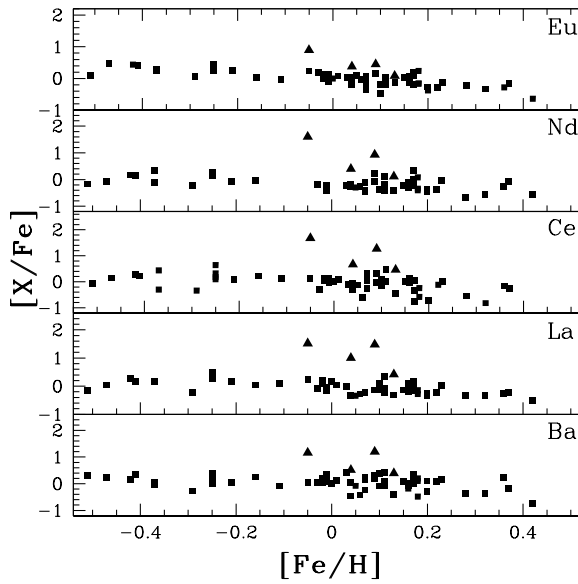
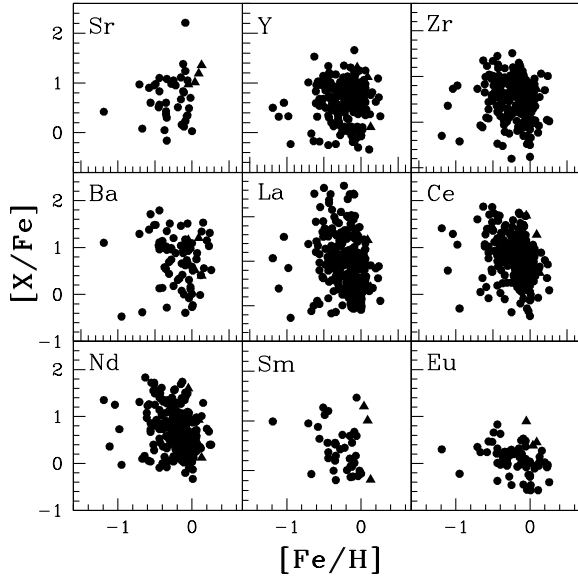


Figure 6. Abundance ratios of heavy elements observed in the programme stars with respect to metallicity $[\text{Fe}/\text{H}]$. The abundance ratios show a large scatter with respect to metallicity. In the upper panel our objects are indicated with solid triangles. Solid circle represents Ba stars from literature (i.e., Allen & Barbuy (2006), Liang et al. (2003), Smiljanic et al. (2007), Zacs (1994), and de Castro et al. (2016).) de Castro et al's data are available only for five heavy elements, Y, Zr, La, Ce and Nd. In the lower panel solid square represents normal giants from literature (i.e., Van der Swaelmen et al. (2016), Tautvaisiene et al. (2000), Luck and Heiter (2007)); our objects are indicated with solid triangles.

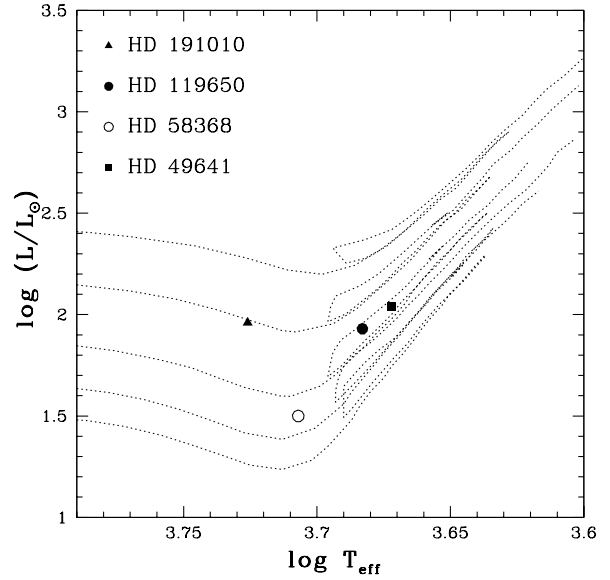


Figure 7. The location of HD 49641, HD 58368, HD 119650 and HD 191010 are indicated in the H-R diagram. The masses are derived using the evolutionary tracks of Girardi et al. (2000). The evolutionary tracks are shown for masses 2.0, 2.2, 2.5, 3.0 and 3.5 M_{\odot} from bottom to top.